INVESTIGATION OF THE CLOSING SHOCK IN A SUPERSONIC SUBMERGED UNDEREXPANDED GAS JET

V. I. Nemchenko

UDC 533.601.172

The geometry of the closing compression shock and the boundary of a submerged underexpanded gas jet are investigated. The self-similarity of the initial section of the jet at high pressures and the disturbance of the self-similarity as the stream density diminishes are shown experimentally.

A study of the structure of an underexpanded jet is of essential value for the further development of the theory of real gas flow and the production of intense molecular beams.

At present there is comparatively little information about the characteristics of the closing shock, particularly at low pressures when the influence of viscosity is substantial, as well as at high Mach numbers at the nozzle section [1-5].

Results of an experimental investigation of the closing shock geometry in the initial section of an underexpanded supersonic jet by the glow discharge method are presented below for different Mach numbers at the nozzle section $1.15 \leq M_a \leq 4.2$, ratios of the pressure at the nozzle section to the pressure in the vacuum chamber $1.7 \cdot 10^1 \leq n \leq 8 \cdot 10^3$, and Knudsen numbers $10^{-4} \leq K_* \leq 10^{-3}$ (the Knudsen number K_* was computed by means of the stream parameters in a critical section of the nozzle). The method of investigation and the low-density wind-tunnel characteristics are described in [6-8]. The geometric nozzle dimensions and the escape modes of a gas jet with diverse adiabatic indices $\gamma = 1.407$ and $\gamma = 1.667$ are given in Table 1, where the upper series in the d column corresponds to the nozzle diameter at the critical section while the lower is the diameter of the nozzle section; S/S_* is the nozzle expansion computed without taking account of the boundary layer; M_a is the Mach number at the nozzle section obtained by means of the results of total head pressure measurements p_0'; p_0 is the pressure in the adiabatically frozen stream in N/m^2; and ξ_0 is the nozzle half-angle. The gas was first heated by an electric heater to a temperature of $T_0 = 523$-$700°K$ to prevent condensation during escape through the supersonic nozzle under conditions of the experiment. Flow visualization in a glow discharge permitted photographing the closing compression shock being formed in the initial section of a strongly underexpanded jet. Results of a visualization of the closing compression shock in air jets issuing from nozzles with different expansion into a space with reduced pressure at high stream densities ($C \sim 10^{-3}$, where $C = K_* \sqrt{n}$ is the rarefaction parameter [4]) are presented in Fig. 1a as an illustration.

On the basis of dimensional analysis and the equations of ideal gas motion it has been shown in [9] that the fundamental geometric dimensions of the initial section of an underexpanded supersonic jet issuing into a space with reduced pressure are self-similar relative to $\sqrt{n}$ and can be determined from dependences of the form

$$\frac{L}{d_a} n^{-1/2} = F(M_a, M_c, \gamma_a, \gamma_c, \xi_0), \tag{1}$$

where d_a is the diameter of the nozzle section; M_c is the Mach number of the satellite flow; and γ_c is the adiabatic index of the satellite flow. This assumes conservation of the ratios D_0/x_0, D/x_0 (x_0 is the position

Institute of Chemical Physics, Academy of Sciences of the SSSR, Moscow. Translated from Inzhenerno-Fizicheskii Zhurnal, Vol. 20, No. 5, pp. 909-917, May, 1971. Original article submitted February 13, 1970.

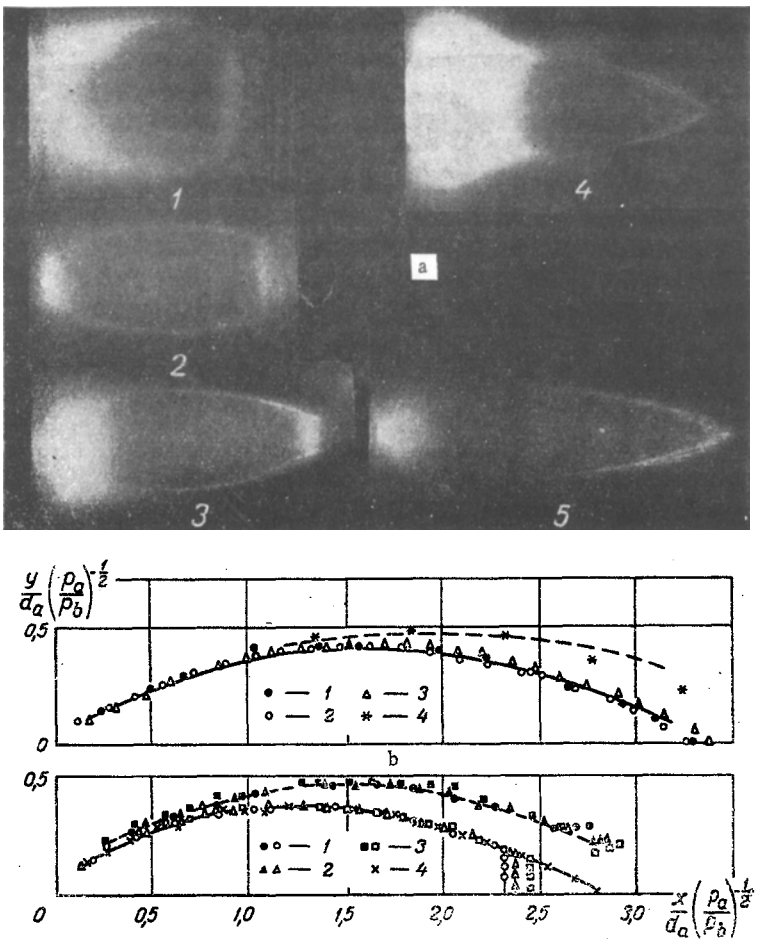

Fig. 1. Geometry of the closing shock in underexpanded supersonic jets: a) photographs of jets visualized in a glow discharge for $K_* \sqrt{n} \approx 10^{-3}$, combinations of the Mach number and pressure ratios [1) 1.15, 945; 2) 2.27, 150; 3) 3.0, 38; 4) 3.3, 41; 5) 3.8, 22.4]; b) results of investigations of the self-similarity of the closing shock and the jet boundary for $M_a = 3.3$ [upper part of Fig. 1b: 1) $K_* \sqrt{h} = 9.4 \cdot 10^{-4}$; 2) $1.96 \cdot 10^{-3}$; 3) $2.3 \cdot 10^{-3}$; 4) $9.4 \cdot 10^{-4}$] and for $M_a = 2.8$ [lower part of Fig. 1b; dark points correspond to the jet boundaries, light points to the hanging shock for the following values of the number $K_* \sqrt{n}$: 1) $K_* \sqrt{h} = 1.13 \cdot 10^{-3}$; 2) $1.48 \cdot 10^{-3}$; 3) $1.69 \cdot 10^{-3}$; 4) $2.02 \cdot 10^{-3}$].

of the closing shock on the jet axis; D_0 is the diameter of the Mach disk; and D is the maximum diameter of the hanging shock), as has been shown earlier experimentally [8, 10]. Conservation of the ratios D_0/x_0, D/x_0 as well as the description of the closing shock geometry by analytical dependences of the form (1) indicates the similarity of the geometry of the jet boundaries and of the closing shock when the quantity $d_a n^{-1/2}$ is used as the characteristic scale. The results of an experimental investigation of the similarity of underexpanded jets with $M_a = 2.8$ and $M_a = 3.3$ are presented in Fig. 1b. The point spread for the different pressure ratios does not exceed the errors of the experiment. There is a completely satisfactory similarity between the hanging shock and the jet boundaries even near the nozzle section $x/r_a \sim 10$. The kinds of jets presented above for different values of M_a (Fig. 1) differ by the nature of the reflection of the hanging shock from the jet axis: for $M_a = 3.0$ irregular reflection with the formation of a Mach configuration occurs under the conditions of the experiment while for $M_a = 3.3$ there is regular reflection with the formation of an x-shock. The angle of incidence ω and the shock intensity $\zeta = p_1/p_2$ determine the process of plane shock reflection [11, 12]. The angle ω is a function of the Mach number at the nozzle section in supersonic jets. Experimental values of the angle of incidence of the hanging shock on the jet axis are given in Fig. 2a for

TABLE 1. Geometric Nozzle Dimensions and Jet Escape Conditions (T_0 = 523-700°K)

$d \cdot 10^3$, m	S/S_*	$\gamma=1,4$ M_a	$\gamma=1,667$ M_a	$P_0 \cdot 10^{-5}$, n/m^2	n	ξ_0
1						
1,01	1,02	1,14		3,99—9,31	10^2—$8 \cdot 10^3$	55′
1,5						
1,95	1,688	1,8		7,05—8,65	78—920	10°
1,85						
3	2,637	2,27	2,5	0,655—9,31	17—785	6° 12′
1,85						
3,35	3,77	2,5	2,81	1,995—9,31	37—10^3	7° 57′
1,85						
3,83	4,235	2,8	3,23	3,99—9,31	20—500	10° 05′
1,5						
3,4	5,121	3,0		599—7,98	30—450	10°
1,5						
4,4	6,79	3,3		3,99—9,31	24—227	10° 20′
1,5						
4,91	10,72	3,8		6,65—7,98	22—180	10°
1,5						
6,09	16,5	4,2		6,65÷8,38	20—123	16° 37′
1,8						
3,83	4,235	2,8		3,99—6,65	36—313	15° 30′
1,8						
3,35	3,77	2,5		3,99—6,65	90—418	15° 30′

$n > 20$ for different M_a and $C \sim 10^{-3}$. When there is no direct intersection of the hanging shock with the jet axis (Mach reflection), the approximation of the hanging shock by the arc of a circle is used to determine the angle ω, which because of the self-similarity of the shock shape introduces no essential errors (see Fig. 1b). A characteristic peculiarity of the process of shock reflection in supersonic underexpanded jets is the high intensity $\zeta < 0.07$ for $n > 20$. Results of investigations of the dependence $\omega = f(M_a)$ for $C \sim 10^{-3}$, $n > 20$ for fixed values of $\gamma = 1.4$, ξ_0 show that the transition from Mach to regular reflection is performed for certain limit values of the angle of incidence ω_l which are similar in value to the limit angle of incidence of a plane high intensity shock $\omega_l = \arcsin 1/\gamma$. Therefore, for a given C there exists a definite Mach number M_{a_l} above which regular reflection occurs. Under these conditions, the behavior of the dependence $\omega = f(M_a)$ permits the extraction of three reflection modes for a hanging shock in supersonic jets; the first mode for $1 \leq M_a \leq 2$ is characterized by high angles of incidence on the jet axis and irregular compression shock reflection, the second mode is for $2 \leq M_a < M_{a_l}$ when the angles of incidence are close to the limit value ω_l but reflection occurs with the formation of a Mach disk, and finally, the third mode is characterized by the angles of incidence $\omega < \omega_l$ and the formation of an x-shock.

If the angle of shock reflection ω' is considered as a function of the angle of incidence ω (i.e., as a function of M_a), then the transition from regular to irregular reflection occurs in a narrow range of M_a variation, where the values of the angles and the nature of the transition agree with the plane case for intense shocks within the accuracy of the experiment (Fig. 2b). The solid lines in Fig. 2b are the results of a theoretical computation $\omega' = f(\omega)$ by means of the theory of regular plane shock reflection [11], the dash-dot lines yield the domain of unrealizable solutions of regular reflection theory, while the dashed lines ($\zeta = 0.8$; $\zeta = 0.2$) are the results of computing the Mach reflection in the plane shock case by means of three-impact theory. The results of the computation by means of the three-impact theory are in good agreement with experiment [13] in the case of intense shocks ($\zeta = 0.2$), where the characteristic singularity is the jump in the function $\omega' = f(\omega)$ near the limiting angle of incidence. This singularity is conserved even in the axisymmetric flow case.

The fundamental hypothesis of the three-impact theory of approximate computation of the Mach configuration is the possibility of describing the motion trajectory of the triple point in plane shock reflection by the equation of a line $y = kx + b'$ and the self-similarity of the flow.

An analogous picture is observed in the Mach reflection case in axisymmetric underexpanded jets. As the pressure ratio n increases, the triple point moves along a ray starting from the center of the source. The slope of the ray relative to the jet axis is determined by the Mach number at the nozzle section for fixed values of M_c, ξ_0. The relationship of the angles in the triple configuration domain is independent of n within the error of the experiment and the motion of the triple point occurs self-similarly. The tangents of the slopes for some M_a are presented in Table 2 for $30 \leq n \leq 5 \cdot 10^2$ and different values of C.

Three-impact wave theory in combination with the method of characteristics was used in [14] to compute the position of the central compression shock and the flow in the Mach configuration domain, which afforded satisfactory agreement between the theoretical and experimental results for the small values $n \approx 10$-20. As n increases the accuracy of the computation in this domain is degraded considerably in connection with the drop in accuracy of the method of characteristics for large x/r_a. The position of the compression shock on the jet axis in the case of nonregular reflection for $M_a < M_{a_l}$ is determined by the empirical dependence proposed in [15]:

$$\frac{x_0}{r_a} = A\sqrt{n}, \tag{2}$$

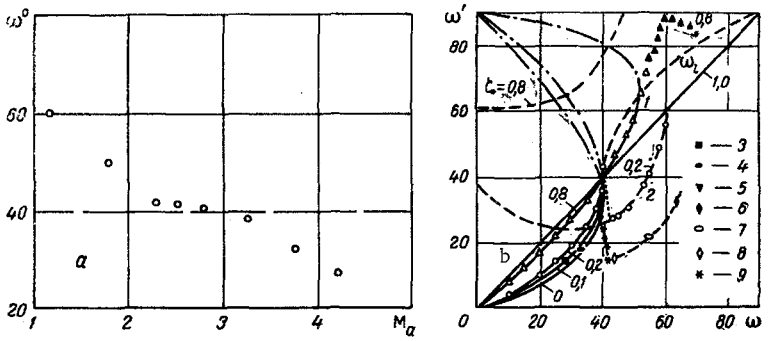

Fig. 2. Dependence of the angle of incidence of a hanging shock on the jet axis on the Mach number M_a at the nozzle section (a) [the dashed line yields the value of the limiting angle of incidence for $\gamma = 1.4$ (plane case)] and the dependence of the angle of reflection of a hanging shock on the angle of incidence (b) [1,2) results from [3], 3-8) results of jet investigations for M_a respectively equal to 4.2, 3.8, 3.3, 2.27, 1.8, 1.15; 9) corresponds to the transition modes for $M_a = 2.8$ and different values of C].

where r_a is the radius of the nozzle exit section and

$$A = 1.38 \sqrt{\gamma}\, M_a. \tag{3}$$

After the passage to the regular reflection which occurs in the narrow band $M_a \approx M_{a_l}$, the position of the x-shock is determined by the dependence (2) but with another proportionality coefficient

$$A_1 = \sqrt{\gamma}\, M_a^{3/2}. \tag{4}$$

The dependences $A = f(M_a)$ (curve 1) and $A_1 = \varphi(M_a)$ (curve 2) are represented in Fig. 3a for $C \sim 10^{-3}$. The dashes yield values of A in the transition domain for different C.

The expression (4) agrees formally with the results of an approximate computation of the position of the point $p_2 = p_b$ on the jet axis by means of the formula proposed in [5].

The diameter of the Mach disk in dense jets ($C \sim 10^{-3}$) depends slightly on M_a in the range $1 \leq M_{a_l} \leq 2.8$ and varies sharply in the transition zone near M_{a_l} (Fig. 3b) where the following dependence can be used to determine its numerical values

$$D_0/d_a = F \sqrt{n}, \tag{5}$$

where $F = F(M_a) \approx 0.5$ in the range $1 \leq M_a \leq 2.8$.

The influence of dissipative processes is superposed on the relations and dimensionalities presented above, which are valid for dense jets ($C \approx 10^{-3}$ in the present trial), as the stream density diminishes for $C > 10^{-3}$. This is naturally manifested most strongly in domain 2 of Fig. 3a, where the angles of hanging shock incidence are close to the limit value. The dissipative processes apparently result in a change in shock intensity [16, 17], which implies a change in the conditions of compression shock reflection from the jet axis. An increase in the angle at the triple point between the hanging shock and the jet axis, and a diminution in the diameter of the Mach disk and its recession from the nozzle section with a subsequent transition into an x-shock as the density diminishes in the incident shock domain ($C > 10^{-3}$) (Fig. 4a) are observed experimentally. The triple configuration was identified with the x-shock if the diameter of the third shock was less than the nozzle diameter. The experimental values of the rarefaction parameter $C = C_1 = f(M_a)$ (for $\gamma = 1.4$) for which disturbance of the ideal flow resulting in diminution of the Mach disk occurs, are given in Fig. 4b. Presented there are experimental values of the parameter $C = C_l = \varphi(M_a)$ ($\gamma = 1.4$, 1.667) at which a transition into an x-shock occurs. An investigation of the boundary of the transition into an x-shock in another gas ($\gamma = 1.667$) for a fixed nozzle half-angle ($\xi_0 = 10°$) has shown that the conditions of the transition in the criterial form of M_a and C depend slightly on the adiabatic index in Fig. 4b.

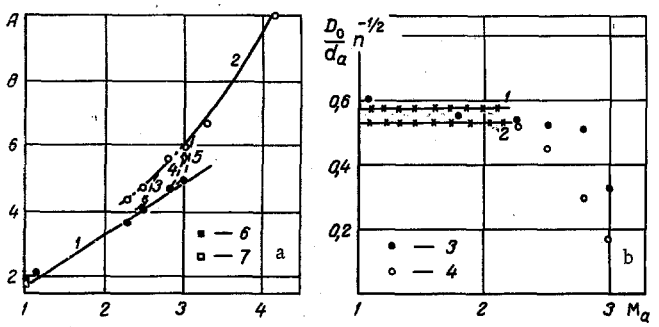

Fig. 3. Distance to the closing shock along the jet axis and diameter of the Mach disk: a) dependence of the coefficients A(1) and A_1(2) on the Mach number at the nozzle section and the rarefaction parameter C (3) $2.5 \cdot 10^{-3}$; 4) $1.5 \cdot 10^{-3}$; 5) $1.0 \cdot 10^{-3}$; 6, 7) data from [1]); b) dimensionless diameter of the Mach disk as a function of M_a [1, 2) results of [1] for $C < 10^{-3}$; 3) $C = 1 \cdot 10^{-3}$; 4) $2 \cdot 10^{-3}$].

TABLE 2. Dependence of the Proportionality Coefficient k on M_a and C

	M_a=2,8				M_a=2,5	
C	1,13·10⁻³	1,48·10⁻³	1,69·10⁻³	2,02·10⁻³	C	1,1·10⁻³
κ	0,117	0,108	0,97	0,82	κ	0,136
	M_a=2,27					
C	2,3·10⁻³	1,72·10⁻³	2,3·10⁻³	4,16·10⁻³	5,27·10⁻³	5,72·10⁻³
κ	0,18 6	0,195	0,186	0,126	0,065	0,03

Within the limits of experimental accuracy it has also been shown that no significant change in the conditions of transition into an x-shock in the criterial form of M_a and C from the nozzle half-angle ($\xi_0 \approx 10$-16°) is observed (Fig. 4b).

As the rarefaction parameter C increases, the diameter of the Mach disk ceases to be described by (5). The results obtained for measurement of the diameter of the Mach disk are not extended when the parameters C, K_{2D} [2] are used, where K_{2D} is computed by means of the flow parameters behind the central compression shock. The extension of the dimensionless Mach disk diameter (more exactly the quantity $(D_0/d_a)n^{-1/2}$) is more satisfactory when the Knudsen number K_{1D} computed along the mean free path of the gas molecules ahead of the Mach disk and its diameter is used as the generalizing parameter. A diminution in the diameter of the Mach disk as compared with the ideal values is observed for $K_{1D} \approx 0.01$-0.02.

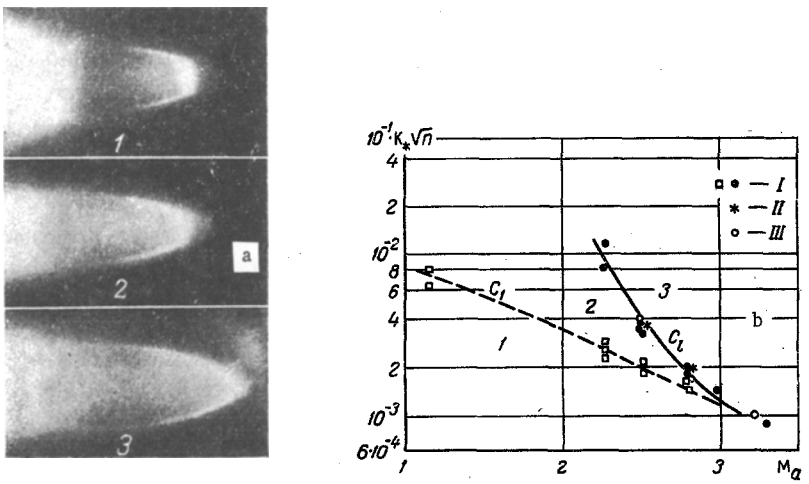

Fig. 4. Results of investigating various kinds of hanging shock reflections from the jet axis: a) change in the nature of reflection as n increases for M_a = 3.0 [1) 31.0, 2) 38, 3) 56]; b) domain of existence of various shock configurations in the neighborhood of the intersection between the closing shock and the jet axis: 1) flow in the Mach configuration domain characteristic for a dense gas jet; 2) transition into an x-shock; 3) domain of x-shock existence [I) air, $\xi_0 \approx 10°$; II) air, $\xi_0 \approx 15°30'$; III) argon, $\xi_0 \approx 10°$].

As has been remarked above, a diminution in the density as C increases results in gradual removal of the central compression shock from the nozzle section and the transition into an x-shock for a fixed Mach number M_a on the nozzle section. The position of an x-shock is determined by (2) with the proportionality coefficient A_1 (4), curve 2 in Fig. 3a in this case. The influence of rarefaction on the behavior of the coefficient A during the transition into an x-shock can be traced well in Fig. 3a, where the dependences of A on M_a are given for three values of C [3) $2.5 \cdot 10^{-3}$; 4) $1.5 \cdot 10^{-3}$; 5) $1 \cdot 10^{-3}$] as a parameter. The values of the limit Mach number M_{a_l} at which the transition into an x-shock occurs are shifted towards lesser M_a as the rarefaction parameter C increases. The width of the band of Mach numbers M_a in which the transition into an x-shock occurs for a fixed value of C depends on M_a, where an increase in the Mach number M_a results in its contraction (Figs. 3a and 4b). A further diminution in the stream density in the domain of the incident compression shock for $C \gg C_l$ causes the approach of the x-shock to the nozzle section [5].

As the rarefaction increases, a change in the slope of the ray describing the trajectory of triple point motion also occurs (see Table 2).

The results presented on the influence of rarefaction on the flow in the Mach configuration domain permit us to say that as the rarefaction increases the disturbance of the self-similarity of the closing shock relative to $\sqrt{n}$ in this domain occurs for fixed Mach numbers. All the changes in the shock geometry presented above in the triple configuration domain become especially graphic in the similarity coordinates $d_a n^{-1/2}$ (Fig. 1b), where C plays the part of the parameter.

NOTATION

p	is the pressure;
T	is the temperature;
γ	is the ratio of specific heats;
ζ	is the shock intensity;
n	is the ratio between the pressure at a nozzle section and the pressure in the vacuum chamber;
M	is the Mach number;
K	is the Knudsen number;
$C = K_* \sqrt{n}$	is the rarefaction parameter;
A, A_1, F	are the proportionality coefficients in empirical formulas describing the closing shock geometry;
S	is the nozzle cross-sectional area;
d	is the nozzle diameter;
r	is the nozzle radius;
ξ	is the half-angle of a conical nozzle;
L	is the geometric closing shock dimension;
x_0	is the distance to the closing shock along the jet axis;
ω	is the angle of incidence of the hanging compression shock;
ω'	is the angle of reflection of the hanging compression shock;
x	is the distance along the jet axis;
y	is the distance across the jet;
k	is the proportionality coefficient;
b'	is some constant.

Subscripts

0	is the parameter in the adiabatically frozen stream;
*	is the parameter in the critical nozzle section;
a	is the parameter at the nozzle exit;
l	is the limit value;
c	is the parameter in the satellite stream;
b	is the parameter in the vacuum chamber.

LITERATURE CITED

1. H. Ashkenas and F. S. Sherman, Rarefied Gas Dynamics, Academic Press, New York–London (1966).
2. K. Bier and O. Hagena, Rarefied Gas Dynamics, Academic Press, New York–London (1963).

3. E. S. Love, C. E. Grigsby, L. P. Lee, and M. I. Woodling, NASA TRR-6 (1959).
4. N. I. Yushchenkova, B. D. Kamaev, S. A. Lyzhnikova, and V. I. Nemchenko, in: Thermophysical Properties of Liquids and Gases at High Temperatures and Plasma [in Russian], Vol. 2, Committee of Standards, Measures, and Measuring Instruments Press, Moscow (1969).
5. N. I. Yushchenkova, S. A. Lyzhnikova, and V. I. Nemchenko, in: Transport Phenomena in a Low-Temperature Plasma [in Russian], Nauka i Tekhnika, Minsk (1969), p. 106.
6. S. I. Kosterin, N. I. Yushchenkova, N. T. Belova, and B. D. Kamaev, Inzh. Fiz. Zh., 5, No. 12 (1962).
7. N. I. Yushchenkova, A. A. Pomerantsev, and V. I. Nemchenko, Int. J. Heat Mass Transfer, 10, 5 (1967).
8. V. I. Nemchenkova and N. I. Yushchenkova, Zh. Prikl. Mekh. i Tekh. Fiz., No. 6, 110 (1969).
9. J. P. Moran, AIAA Journal, 5, 1343 (1967).
10. S. Crist, P. M. Sherman, and D. K. Glass, AIAA Journal, 4, No. 1, 68 (1966).
11. Principles of Gas Dynamics [Russian translation], IL, Moscow (1963).
12. T. V. Bazhenova, L. G. Gvozdeva, Yu. S. Lobastov, I. M. Naboko, R. G. Nemkov, and O. A. Predvoditeleva, Shock Waves in Real Gases [in Russian], Nauka, Moscow (1968).
13. R. Kawamura and H. Saito, J. Fluid Mechanics, 2, No. 5 (1957).
14. D. Attore and Harshbarger, Raketnaya Tekhnika i Kosmonavtika, 3, No. 8, 196 (1965).
15. C. H. Lewis, Jr. and D. J. Carlson, AIAA Journal, 2, No. 4, 776 (1964).
16. A. V. Ivanov, Dokl. Akad. Nauk SSSR, 161, No. 2 (1965).
17. V. V. Volchkov and A. V. Ivanov, Izv. Akad. Nauk SSSR, Mekhan. Zhidk. i Gaza, No. 3, 160 (1969).